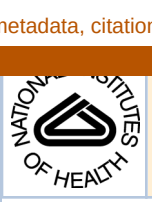

Published in final edited form as:

Biochemistry. 2012 January 31; 51(4): 888–898. doi:10.1021/bi2018078.

Hsp70 alters tau function and aggregation in an isoform specific manner†

Kellen Voss[1], **Benjamin Combs**[1], **Kristina Patterson**[2], **Lester I. Binder**[2], and **T. Chris Gamblin**[1,§]

[1]Department of Molecular Biosciences, University of Kansas, 1200 Sunnyside Avenue, Lawrence, KS 66045, USA

[2] Department of Cell and Molecular Biology, Feinberg School of Medicine, Northwestern University, Chicago, Illinois 60611

Abstract

Tauopathies are characterized by abnormal aggregation of the microtubule associated protein tau. This aggregation is thought to occur when tau undergoes shifts from its native conformation to one that exposes hydrophobic areas on separate monomers, allowing contact and subsequent association into oligomers and filaments. Molecular chaperones normally function by binding to exposed hydrophobic stretches on proteins and assisting in their refolding. Chaperones of the heat shock protein 70 (Hsp70) family have been implicated in the prevention of abnormal tau aggregation in adult neurons. Tau exists as six alternatively spliced isoforms, and all six isoforms appear capable of forming the pathological aggregates seen in Alzheimer's disease. Because tau isoforms differ in primary sequence, we sought to determine whether Hsp70 would differentially affect the aggregation and microtubule assembly characteristics of the various tau isoforms. We found that Hsp70 inhibits tau aggregation directly, and not through inducer mediated effects. We also determined that Hsp70 inhibits the aggregation of each individual tau isoform and was more effective at inhibiting the three repeat isoforms. . Finally, all tau isoforms robustly induced microtubule formation while in the presence of Hsp70. The results presented herein indicate that Hsp70 affects tau isoform dysfunction while having very little impact on the normal function of tau to mediate microtubule assembly. This indicates that targeting Hsp70 to tau may provide a therapeutic approach for the treatment of tauopathies that avoids disruption of normal tau function.

The microtubule associated protein tau exists as six isoforms generated by alternative splicing at exons 2, 3, and 10 (*1*, *2*). Splicing of the amino-terminal exons 2 and 3 results in isoforms possessing either zero (0N), one (1N) or two (2N) N-terminal inserts. Exon 10 encodes for one of four functional microtubule binding repeats (MTBRs) located near the carboxyl-terminus. Alternative splicing at exon 10 results in isoforms possessing either 3 or 4 repeats (3R or 4R, respectively). Tauopathies are a class of neurodegenerative disorders that arise from the misfolding of tau protein, resulting in its aggregation into amyloid fibrils (reviewed in (*3*)). Changes in the alternative splicing of tau have been associated with tauopathies such as progressive supranuclear palsy (PSP) and corticobasal degeneration

---

†Support was provided by NIH T32 AF020506 (KRP); NIH AG09466, AG032091 (LIB); NIH AG022428, AG025898 (TCG) and the J.R. and Inez Jay Fund (TCG)

§Corresponding Author: T. Chris Gamblin Department of Molecular Biosciences University of Kansas 1200 Sunnyside Ave. Lawrence, Kansas 66045 Telephone: (785)-864-5065 Fax: (785) 864-5321 gamblin@ku.edu.

SUPPORTING INFORMATION AVAILABLE

Additional data describing controls for the ARA, CR and heparin induction of tau aggregation in the presence of Hsp70 are provided in Supplemental Figures 1-4. Electron micrographs of aggregate clumping and the effects of Hsp70 on aggregate clumping are provided in Supplemental Figure 5. This material is available free of charge via the Internet at http://pubs.acs.org.

(CBD), which have an increase in 4R tau. By contrast, Pick's disease generally has an increase in 3R tau (reviewed in (*4*)). However, in Alzheimer's disease (AD), tau isoform ratios are somewhat controversial with multiple reports of no differences in splicing between AD and controls (*5-10*) and multiple reports of altered splicing ratios (*11-16*). These differences in observations are likely due to the difficulty and technical limitations of the experimental approaches employed. However, it is also likely that in addition to any potential changes in altered isoform ratios, post-translational modifications of isoforms and their interactions with other cellular proteins could play a major role in pathogenesis. We have shown previously that tau isoform aggregation is affected by the buffer conditions, the type of inducer for aggregation used, and post-translational modifications (*17*). The aggregation differences caused by changes in the local environment indicate that each isoform may have a distinct role in the aggregations process leading to neurodegeneration.

In neurodegenerative tauopathies, molecular chaperones such as the heat shock proteins are believed to play a significant role in reducing the accumulation of abnormal tau (reviewed in (*18*)). Molecular chaperones have multiple roles, including the prevention of inappropriate aggregation of hydrophobic regions of misfolded proteins, targeting proteins to subcellular compartments, and assisting in degradation of proteins (reviewed in (*19*)). In the central nervous system, Hsp70 levels are normally low but expression of the protein is increased in response to stresses such as hypoxia, elevated temperature, inflammation, and other insults (reviewed in (*20*)). Hsp70 functions by binding exposed hydrophobic regions of proteins via its substrate-binding domain while its ATPase domain hydrolyzes ATP to ADP, creating a higher affinity interaction with the substrate (reviewed in (*21*)). Hsp70 can then directly assist in protein refolding, transfer the protein to the heat shock protein 90 (Hsp90) system, or transfer the protein to the chaperonin system for refolding (reviewed in (*21*)).

Elevated levels of stress response proteins have been observed in AD (reviewed in (*18*)), leading to an increased focus on the role of chaperones in the disease state. Elevated protein levels of Hsp70/90 have been observed in hippocampal sections from AD patients as compared to aged matched controls (*22-24*). In specific hippocampal neurons there is an inverse relationship of tau aggregation and Hsp70/90 levels (*23*). Moreover, in both animal and cellular models, the expression of Hsp70 has been shown to reduce the levels of abnormal tau (*23, 25*). The Hsp70 family member, heat shock cognate 70 protein (Hsc70), has been shown to bind tau directly *in vitro* (*26*), and multiple studies have observed a tau/Hsp70 interaction *in vivo* (*23-27*). Although the constitutively expressed Hsc70 is more abundant and has been shown to be involved in tau processing in aging and neurodegenerative diseases (*28*), we have chosen to focus this study on Hsp70 because of its inverse relationship with tau pathology and its ability to reduce abnormal tau levels in models of neurodegeneration. Likewise, although it is known that Hsp70 activity is greatly enhanced by co-chaperones such as J-proteins and nucleotide exchange factors (NEFs) (*29*), we have chosen to focus this initial study on the intrinsic ability of Hsp70 to influence tau function in the absence of ATP cycling. Due to the large number of J-proteins and NEFs that could play a role in modulating Hsp70 activity toward tau, these important questions will be the focus of future research efforts.

Previous work studying Hsp70/tau interactions has shown Hsp70 reduces abnormal tau aggregation (*24, 30*). However, tau exists as six isoforms that are known to have differing propensities for microtubule-binding and aggregation (reviewed in (*31-37*)). Furthermore, it is likely that the inclusion or exclusion of exons 2, 3 and 10 could alter the overall conformation of tau, perhaps affecting the availability of the microtubule-binding repeats. Lastly, it has been observed that the microtubule binding repeats are the major sites for microtubule binding (*38-40*), tau aggregation (*41, 42*) and heat shock protein interactions (*26*). Based on this evidence, we sought to determine whether Hsp70 would differentially

affect the aggregation and microtubule assembly properties of the individual tau isoforms *in vitro*.

In this study, we demonstrate that Hsp70 inhibits tau aggregation *in vitro* but has varying effects on individual tau isoforms. Additionally, Hsp70 had differential, but minor effects on the nucleation and stabilization of microtubules by the individual tau isoforms. These results suggest that Hsp70 is effective in inhibiting the aggregation of all six isoforms of tau while maintaining the ability of tau to stabilize microtubules, providing biochemical evidence that the up-regulation of Hsp70 may afford protection against tau-induced neurodegeneration.

EXPERIMENTAL PROCEDURES

Protein purification

WT tau isoforms (2N4R, 2N3R, 1N4R, 1N3R, 0N4R, and 0N3R) cloned into a PT7c vector with an N-terminal polyhistidine tag have been previously described (*17, 26, 43*). Hsp70 (*HSPA1A*) (Open Biosystems) was cloned into a pET28b vector (Novagen) with an N-terminal polyhistidine tag. Proteins were expressed in *E. coli* and purified by nickel affinity chromatography using Chelating Sepharose Fast Flow (GE Healthcare) followed by size exclusion chromatography on a Superdex 200 column using an ÄKTA FPLC (GE Healthcare) as previously described (*17*). Protein concentration was determined by a commercially available BCA kit (Pierce), and the purity of each protein was assayed by electrophoresis of microgram amounts on SDS-PAGE gels followed by staining with Coomassie Brilliant Blue R-250.

Tau aggregation with Arachidonic Acid, Congo Red, and Heparin

Tau isoforms (2-4μM) in 10 mM Hepes pH 7.64, 100 mM NaCl, 0.1 mM EDTA and 5 mM DTT were incubated with either arachidonic acid (ARA) or Congo red (CR) to induce aggregation (*17, 44-49*). BSA (0.25 μM) was added to prevent aggregate clumping at higher temperatures. There were no significant differences in the detected amount of polymerization between tau aggregation reactions performed with or without BSA (data not shown). All reactions were carried out at 37 °C for 18 hours. ARA (Cayman Chemicals; 90010.1) was diluted to a final concentration of 75-150 μM, and the concentration of ethanol carrier was kept constant at 3.75%. Congo red (CR) (Sigma; C6277) was dissolved in water and used at a final concentration of 10 μM in aggregation buffer (*45, 50*). Alternatively, heparin (Sigma; H4784; estimated molecular weight between 6-30 kDa) was dissolved in water and used at a final concentration of 6 μg/ml to induce 2N4R tau (2 μM) aggregation in low salt buffer (30 mM Hepes pH 7.64, 18 mM NaCl and 5 mM DTT) (*17, 44, 51*). For inhibition studies, Hsp70 (0-2 μM) was added to aggregation reactions containing ARA, CR or heparin as described above. No differences were observed between his-tagged Hsp70 and non-his-tagged Hsp70 (data not shown). Aggregation was assayed using right angle laser light scattering (LLS), thioflavin S fluorescence (ThS), and transmission electron microscopy (TEM) similar to that previously described (*44*) with the following changes: the laser used for LLS was a 12 mW solid state 532 nm laser operating at 7.6 mW (B&W Tek) and the electron microscope used was a Tecnai F20 XT Field Emission TEM (FEI). The concentration of Hsp70 required to achieve 50% maximal inhibition was determined using GraphPad Prism by plotting the percent aggregation (normalized to the largest and smallest data points in each set) versus the log([Hsp70]) and fitting to an inhibitory dose response curve with variable slope:

$$Y=100/\left(1+10^{(\log IC50-X*HillSlope)}\right)$$

Where X is the log of concentration of Hsp70 in μM, Y is the normalized response (decreasing from 100% (no inhibition) to 0% (complete inhibition) with increasing Hsp70 concentrations), log(IC_{50}) is in the same log units as Hsp70 concentration and is the Hsp70 concentration required to achieve 50% of its inhibitory effects, and HillSlope is the steepness of curve from no inhibition to maximal inhibition.

Tau aggregation in the presence of ATP and Hsp70

4 μM 2N4R tau aggregation reactions with 150 μM ARA was performed as described above. Hsp70 was included at a final concentration of 1 μM either with 500 μM ATP or with 500 μM ATPγS. Hsp70 without nucleotide added was performed as a control. Reactions were incubated for 18 hrs at 37 °C and aggregation was measured by ThS fluorescence. Differences between reactions were compared using a t-test.

Hsp70 disassembly of pre-formed tau aggregates

4 μM 2N4R tau aggregation reactions were performed in polymerization buffer with 0.25 μM BSA, 150 μM ARA at 37 °C. After 6 hrs incubation, Hsp70 was added to the reaction at a final concentration of 1 μM without ATP or at a final concentration of 2 μM Hsp70 and 2 mM ATP. An equal volume of buffer was added to a control reaction to account for dilution effects. The reactions were incubated for a further 18 hrs and the amount of aggregated material was measured by TEM for aggregate lengths and analyzed as described below.

Aggregate length distribution analysis of transmission electron microscopy (TEM) images

TEM images were analyzed for aggregate lengths using previously published protocols (*52*), with the exception that Image Pro Plus 6 (Media Cybernetics) was used for quantitation. Images were set to a threshold that included electron dense aggregates, but any non-specific background material or dense material that did not meet user defined criteria for length and area were ignored. Control samples containing 2 μM Hsp70 in the absence of tau were used to determine background levels of Hsp70 aggregation (*53, 54*). Only objects that were longer than 25 nm, and having an area greater than 375 nm^2 (25 nm long and 15 nm wide) were included in the quantitative analysis, similar to previously published protocols for quantitative electron microscopy of tau aggregates (*55*). The length of each aggregate from five images per reaction were determined for each isoform at three different Hsp70 concentrations: 1) no Hsp70, 2) a concentration of Hsp70 close to the IC_{50}, and 3) a concentration of Hsp70 that resulted in maximal inhibition of tau aggregation. The resulting aggregate lengths were transformed to a log scale and a frequency distribution was performed using GraphPad Prism. The data was fit to a Gaussian equation and tested for significant differences using a global fit comparison sum-of-squares F test.

Microtubule assembly

Microtubule assembly assays were performed using a commercially available DAPI fluorescence based porcine tubulin polymerization assay kit (Cytoskeleton), according to the manufacturer's protocol for detecting enhancers of tubulin assembly in the absence of glycerol or paclitaxel (*56, 57*). Reactions were performed using 1 μM tubulin and 1 μM tau either with or without 1 μM Hsp70. Reactions were incubated at 37 °C and readings were taken every minute for one hour duration using a Molecular Devices Flexstation II plate reader with an excitation wavelength of 355 nm and an emission wavelength of 460 nm. Tubulin assembly reactions (without tau) containing 1 μM taxol alone, 1 μM Hsp70 alone and tubulin alone were used as controls.

Data for microtubule assembly reactions were normalized to 1 μM taxol stabilized microtubule reactions run in parallel to adjust for variability in tubulin assembly with the

background reading set to a value of zero and the maximum amount of fluorescence observed set to a value of 1. Reactions for isoforms with and without Hsp70 were always performed at the same time and with the same aliquot of tubulin to ease comparisons. Normalized data was fit to a Gompertz growth curve (*58, 59*) , defined as:

$$Y=ae^{-e^{-\frac{x-c}{b}}},$$

where *Y* is the relative fluorescence level, *a* is the maximum amount of fluorescence, *x* is time, *b* is $1/k_{app}$ where k_{app} is proportional to the rate of assembly, and *c* is the point of greatest increase in *Y*. Lag time to significant assembly (calculated by *c*-*b*), k_{app} and maximum assembly (*a*) were determined from independent trials with or without Hsp70 and are represented as the mean ± SD.

Fitting Hsp70 inhibition data to binding models

The inhibition curves of 3R tau aggregation by different concentrations of Hsp70 were fit by a single site binding equation:

$$\nu=\frac{B_{max}(K_1[A])}{1+K_1[A]},$$

where ν is the fraction of tau bound by Hsp70, B_{max} is maximal binding, K_1 is the association constant for binding and A is the amount of free Hsp70. The experimental inhibition curves were fit manually by adjusting the values of B_{max} and K_1 assuming that inhibition is directly proportional to binding of Hsp70.

The inhibition curves of 4R tau aggregation by different concentrations of Hsp70 were fit by a two site binding equation:

$$\nu=\frac{B_{max}\left(2K_2[A]+2K_2^2[A]^2\right)}{1+2K_1[A]+K_2^2[A]^2},$$

where ν is the fraction of tau bound by Hsp70, B_{max} is maximal binding, K_1 is the association constant for binding to the first site, K_2 is the association constant for the second site and A is the amount of free Hsp70. The values B_{max} of K_1 were kept the same as the fits for 3R isoforms. The inhibition curves were fit manually by adjusting the values for K_2 assuming that inhibition was directly proportional to the amount of tau with two Hsp70 bound (tau bound by a single Hsp70 would not be inhibited for 4R isoforms).

RESULTS

Hsp70 inhibits 2N4R tau aggregation directly

We sought to confirm that Hsp70 inhibits tau aggregation *in vitro* by using a variety of aggregation inducers. The inducers arachidonic acid (ARA) (*60*), heparin (*61*), and Congo red (CR) (*45*) were chosen for their structural diversity. Full-length 2N4R tau was incubated with ARA and varying concentrations of Hsp70 for 18 hours and the resulting amount of aggregation was assayed by laser light scattering (LLS) (Figure 1A), thioflavin S (ThS) (Figure 1B) and transmission electron microscopy (TEM) (Figure 1C-E). The data was background corrected using reactions that were similar to each concentration of Hsp70, but lacked tau (Supplemental Figure 1). At low concentrations of Hsp70, there was little

observable effect. However, increasing the concentration of Hsp70 reduced the amount of tau aggregation observed. Maximal inhibition was observed at a 2:1 molar ratio of tau to Hsp70. The higher concentrations of Hsp70 causing a decrease in overall tau aggregation also caused a noticeable decrease in aggregate lengths (Figure 1D, E) in comparison to controls lacking Hsp70 (Figure 1C).

Hsp70 was also added to CR induced tau aggregation reactions at varying concentrations and analyzed by LLS (Figure 2A) and TEM (Figure 2B-D). The data was background corrected using reactions that were similar to each concentration of Hsp70, but lacked tau (Supplemental Figure 2). The amount of tau aggregation detected by LLS decreased significantly with increasing concentrations of Hsp70 (Figure 2A). Additionally, a decrease in aggregate lengths and an increase in the number of aggregates observed per field was seen with increasing Hsp70 concentrations (Figure 2C, D) as compared to reactions without Hsp70 (Figure 2B). Hsp70 was also added to heparin sulfate induced tau aggregation reactions and analyzed by ThS (Figure 3A) and TEM (Figure 3B-D). Similar to the ARA and CR, the data was background corrected using reactions that were similar to each concentration of Hsp70, but lacked tau (Supplemental Figure 3). Again, increasing the concentration of Hsp70 dramatically decreased the amount of tau aggregation (Figure 3A). Visualization of samples by TEM without Hsp70 revealed only very long aggregates (Figure 3B). These aggregates were so long that the ends did not fit into a 6 μm by 6 μm field of view. Upon addition of Hsp70, aggregate lengths decreased and the number of aggregates observed per field increased (Figure 3C, D). Electron micrographs of each Hsp70 concentration showed with increasing concentrations of Hsp70, the aggregate lengths began to shorten (Supplemental Figure 4). Together, these data indicate that Hsp70 decreases tau aggregation independent of the inducer employed despite the fact that these compounds (ARA, CR and heparin) are structurally distinct.

Hsp70 can act in an ATP independent manner to inhibit tau aggregation

Hsp70 normally functions by hydrolyzing ATP to ADP in the ATPase domain to enhance the association with a ligand. We therefore sought to determine whether the addition of ATP would affect Hsp70 inhibition of tau aggregation. As expected, the addition of ATP and a non-hydrolyzable analog ATPγS reduced the Hsp70 inhibition of tau aggregation at two different tau concentrations (Figure 4A-D). The presence of ATP reduces the affinity of Hsp70 for its client proteins and the lack of co-chaperones or nucleotide exchange factors greatly reduces the ATPase activity and cycling to the higher affinity ADP + phosphate state. The similarity between ATP and the non-hydrolyzable analog ATPγS strongly suggests that this is the case. We therefore sought to determine whether the ATP inhibition of Hsp70 could be overcome by increasing the concentration of Hsp70 with respect to tau. Increasing the concentration of Hsp70 to 1 μM in the presence of 2 μM tau greatly reduced the effect of ATP on the inhibition of tau aggregation (Figure 4E-F).

The occasional disagreement between ThS and LLS results (compare Figure 4C with Figure 4D) can indicate a difference in filament morphologies. We therefore examined the aggregation morphologies by electron microscopy. We found that the addition of ATP to tau in the absence of Hsp70 (Figure 5C, D) increased the frequency of smaller aggregates as compared to tau alone (Figure 5A, B), despite similar levels of overall aggregation as determined by ThS fluorescence. We also observed that tau incubated with Hsp70 (Figure 5E, F) or Hsp70 and ATP (Figure 5 G, H) had similar aggregate frequency distributions, despite being significantly different by ThS fluorescence measurements. Finally, we observed that the addition of ATPγS and Hsp70 (Figure 5I, J) had fewer aggregates overall, as indicated by the lower amplitude frequency distribution of small aggregates when compared to tau aggregated with Hsp70 (Figure 5E,F) or Hsp70 and ATP (Figure 5G, H). While it is clear that nucleotide addition is having an effect on Hsp70 inhibition of tau

aggregation, it should be noted that in the future similar experiments with co-chaperones and nucleotide exchange factors will be required for a full understanding of the role of nucleotides in this process.

Hsp70has modest effects on pre-formed tau aggregates

We have shown that Hsp70 can prevent aggregation of tau when added at the beginning of the reaction. While Hsp70 is not known to break apart aggregates of protein, it could potentially aid in this process by removing tau from the ends of pre-formed aggregates. We therefore added Hsp70 to preformed tau aggregates and assessed changes in filament morphologies. 2N4R tau was aggregated in the presence of ARA for 6 hrs. Either buffer alone (Figure 6A, B), 1 μM Hsp70 alone (Figure 6C, D), or 1 μM Hsp70 and 2 mM ATP (Figure 6E, F) was added to separate reactions, incubated for an additional 12 hrs, and visualized by TEM. The lengths of the individual aggregates were determined, converted to log scale and summarized as a frequency distribution. The addition of Hsp70 to pre-formed aggregates resulted in a reduction of longer aggregates and an increase in the frequency of smaller aggregates (compare the dashed fit of 2N4R tau alone to the solid fit of 2N4R tau + Hsp70, Figure 6D). The combination of Hsp70 and ATP added to pre-formed aggregates resulted in a further reduction in longer aggregates and a concomitant increase in shorter aggregates (Figure 6E, F), suggesting the possibility that nucleotides could play a role in the Hsp70 disassembly of pre-formed tau filaments. These results are consistent with previous results that Hsp70 has only modest effects on pre-formed tau filaments (*30*).

Hsp70 differentially inhibits aggregation of individual tau isoforms

Tau exists as six alternatively spliced isoforms that differ in primary sequence, with 2 alternatively spiced exons in the amino terminal region of tau and another alternatively spliced exon near the carboxy terminus (Figure 7A). The absence of MTBR2 in 3R isoforms causes a decrease in microtubule binding ability and overall aggregation potential in the presence of ARA as compared to 4R isoforms (*17, 39, 40, 52*). We therefore sought to determine whether Hsp70 would have disparate effects on the aggregation of the tau isoforms. The six individual tau isoforms (4 μM) were induced to aggregate using ARA in the presence of varying concentrations of Hsp70. The extent of aggregation was determined using LLS (Figure 7B) and ThS (Figure 7C). Hsp70 inhibited ARA-induced aggregation of each tau isoform in a dose-dependent manner, but the inhibition curves were different. In the presence of low Hsp70 concentrations (less than 0.25 μM Hsp70) there was a dramatic decrease in aggregation for 3R isoforms while 4R isoforms were largely unaffected at this concentration. 3R isoforms were almost maximally inhibited at higher Hsp70 concentrations that only inhibited 4R isoforms by approximately 50%. 3R tau containing both N-terminal inserts (2N3R) was inhibited at lower concentrations of Hsp70 as compared to 0N3R and 1N3R. In comparison, Hsp70 affected all three 4R isoforms similarly. The IC_{50} for each tau isoform is reported in Table 1.

Inhibition of the aggregation of different tau isoforms was confirmed using TEM (Figure 8). Hsp70 was used at a concentration corresponding to half maximal and maximal inhibition levels. In general, the addition of Hsp70 resulted in a decrease in the number of longer aggregates and a concomitant increase in the number of shorter aggregates as indicated by an increase in amplitude and shift in maxima to the left with the addition of Hsp70 (Figures 8C, F, I, L, O, R). The 3R isoforms were inhibited at lower concentrations of Hsp70 than what was observed for 4R isoforms. There were subtle differences in the patterns of inhibition, but these seem small in comparison to the effect of the extra MTBR, suggesting the likelihood that the N-terminal repeats do not play a large role in modulating Hsp70 interactions with tau. The frequency distributions for the 0N4R isoform are more difficult to interpret due to aggregates clumping in the absence of Hsp70 (Supplemental Figure 5). The

results for all the tau isoforms indicate that there is a general inhibition of aggregate elongation and are consistent with Hsp70 differentially affecting the tau isoforms.

Hsp70 has modest effects on tau-stimulated microtubule assembly

Tau is a microtubule associated protein and previous work has shown that Hsp70 increases the affinity of tau for microtubules in cultured cells (*23*). We therefore sought to determine whether Hsp70 influences tau-stimulated microtubule assembly by incubating each tau isoform with and without Hsp70 in the presence of tubulin (Figure 9). The ratio of tau to Hsp70 employed (1:1 ratio) was enough to achieve maximal inhibition of tau aggregation *in vitro* (see Figure 7). The lag time, maximum amount and rate of microtubule assembly were determined for each isoform in the presence and absence of Hsp70 by fitting the data to a growth curve. The buffer only and Hsp70 only in the absence of tau both show no stimulation of microtubule assembly (Figure 9F). Each isoform robustly stimulated microtubule assembly in the presence and absence of Hsp70 (Figure 9A-F), although some significant differences in the presence of Hsp70 were observed (Table 2). Two isoforms had changes in the maximum amount of tubulin assembly (2N3R, 0N4R), two isoforms were significantly altered in all three kinetic parameters (0N3R, 1N4R) and two isoforms were not significantly affected by Hsp70 (2N4R, 1N3R). However, the changes observed seemed minor in comparison to the degree of inhibition of tau isoform aggregation caused by Hsp70 (see Figures 7 and 8).

DISCUSSION

Expression of Hsp70 is elevated in AD, possibly in response to oxidation and inflammatory events (*63-67*). The inverse relationship of Hsp70 expression and tau pathology in hippocampal neurons suggests that the up-regulation of Hsp70 is protective against abnormal and aggregated tau. Previous studies demonstrated that higher levels of Hsp70 in cultured cells can decrease the levels of insoluble 0N3R or 2N4R tau and increase their association with microtubules (*23*). Due to these and other observations of interactions between tau, Hsp70 or Hsp70 family members (*23-27*), we sought to determine whether Hsp70 was a general inhibitor of tau aggregation *in vitro*. The aggregation of 2N4R tau induced by any of three different compounds (ARA, CR or heparin) was significantly inhibited in the presence of Hsp70. The ability of Hsp70 to reduce the aggregation induced by such structurally distinct molecules strongly suggests that Hsp70 inhibition is not inducer specific, but rather specific to tau, bolstering its potential as a neuronal inhibitor of tau aggregation. While a strong argument can be made for a biological role for ARA in the induction of tau aggregation in AD (*68*), it is currently unknown whether *in vivo* tau aggregation requires an inducer or what the nature of that inducer may be. We have demonstrated that Hsp70 can inhibit tau aggregation triggered by a wide variety of inducer molecules, suggesting that Hsp70 is a general inhibitor of tau aggregation, perhaps capable of blocking most tau inducers or aggregation in the absence of inducers.

Although Hsp70 is highly effective at preventing the aggregation of 2N4R tau *in vitro (30)*, very little was known about its effect on the other isoforms of tau that arise from alternative splicing. Several factors suggest that the interaction between Hsp70 and tau isoforms may not be the same. First, one of the putative Hsp70-binding sites is believed to be located adjacent to the second MTBR, a region absent in 3R isoforms (*26*). Secondly, tau is believed to adopt a global hairpin conformation in solution in which the amino terminus folds over to come in close proximity to the carboxy terminal tail and the MTBRs (*69*). Exons 2 and 3 reside near the N-terminus and the presence or absence of these exons may influence the folding of this region and, thus, the formation of the hairpin conformation. We therefore sought to determine whether Hsp70 would differentially influence the aggregation of tau isoforms. To this end, we demonstrated that Hsp70 was more effective in inhibiting the

aggregation of 3R isoforms and that the N-terminal exon 3 had only a small effect in the 3R isoforms and none in the 4R isoforms.

One potential mechanism that would explain the increased inhibition of 3R isoforms as compared to 4R isoforms can be deduced from the inhibition data. If we assume that the decrease in polymerization is directly proportional to the amount of bound Hsp70, we can treat the inhibition curves as binding isotherms (Figure 10). Unfortunately, the 3R and 4R inhibition curves cannot be adequately approximated by a single binding equation. However, previous results have shown that a constitutively expressed heat shock protein, Hsc70, which shares approximately 90% sequence identity with Hsp70, can bind to tau isoforms at two separate sites (^{275}VQIINK^{280} and ^{306}VQIVYK^{311}, hexapeptide motifs located in exon 10 and near MTBR3, respectively). We therefore used a single-site model to fit 3R inhibition and a 2-site model to fit 4R inhibition. The fit of the data was greatly improved by assuming that Hsp70 is binding to an oligomer (i.e. max binding is less than 1), which is consistent with our previously published report (*30*). The 4R data was better fit to the 2-site binding equation assuming that the second site is lower affinity than the first and that only tau molecules that are doubly occupied are inhibited (Figure 10). The following inferences can therefore be drawn from fitting the data to these equations: a) It is likely that the site of Hsp70 inhibition is at the end of the aggregate, preventing the addition of new tau molecules onto the growing end; b) binding could occur before or after addition to the growing aggregate, but it is the act of blocking the next oncoming tau to the end that results in inhibition; and c) 4R tau with a single Hsp70 bound could still use its second unbound aggregation site to participate in the aggregation process and allow another tau molecule to add to the end.

While results indicate that the inhibition of tau aggregation can occur without hydrolysis of ATP, we cannot fully address the role of ATP hydrolysis in Hsp70 inhibition of tau aggregation in the current study. It seems likely that Hsp70 is not cycling through ATP hydrolysis and exchange due to the lack of co-chaperones and nucleotide exchange factors. The similarity in results between ATP and ATPγS also indicates that ATP cycling is not required for Hsp70 inhibition of tau aggregation. It is likely that the co-chaperones such as Hsp40 and nucleotide exchange factors such as BAG-1 will have a large impact on the function of Hsp70 and its regulation of tau aggregation. It is also just as likely that other chaperones with similar functions to Hsp70 could also inhibit tau aggregation. Our current study provides a benchmark for future analyses of chaperone/co-chaperone inhibition of tau aggregation. It is potentially significant that Hsp70 is capable of protecting tau from aggregation without the need for ATP hydrolysis and cycling given the high degree of mitochondrial dysfunction and altered metabolism present in the brains of Alzheimer's patients (*70*). The observation that Hsp70 can serve a protective role even in suboptimal energetic conditions is encouraging as one considers potential therapeutic applications.

The predicted sites of Hsp70 binding are located with the MTBR region, thereby raising the possibility that Hsp70 binding to this region could inhibit the normal functions of tau through steric hindrance. Previously, it was demonstrated that increased Hsp70 expression levels in cultured cells resulted in the increased association of tau with microtubules. This indicates Hsp70 does not interfere with the ability of tau to associate with microtubules. However, phosphorylation of tau can significantly decrease its stabilization of microtubules while maintaining substantial interactions with preformed microtubules (*71*). We therefore sought to determine whether Hsp70 would affect the microtubule nucleation and stabilization properties of tau isoforms. Even in the presence of equimolar concentrations of Hsp70, tau isoforms robustly assembled microtubules. However, Hsp70 did significantly affect the amount of time required to begin to polymerize tubulin (lag time), depressing both the rate of microtubule assembly and the steady state levels of microtubule assembly in the

presence of 0N3R and 1N4R tau. 0N4R and 2N3R also had significantly reduced levels of microtubule assembly, while 1N3R and 2N4R were unaffected by Hsp70. There does not appear to be a consistent pattern of exon incorporation that correlates with the effects of Hsp70 on tau function. This could indicate that the interaction of Hsp70 with tau isoforms is complicated by their different conformational states. However, it should be noted that the largest changes observed, though significant, represent only a 29% increase in microtubule assembly rate and a 30% decrease in microtubule lag time in the presence of 1N4R. Therefore, while our data demonstrate that Hsp70 acts specifically on certain isoforms to change their ability to associate with microtubules, all maintain their ability to stabilize microtubules and the observed changes are small in comparison to the observed effects of Hsp70 inhibition of tau aggregation.

In conclusion, we demonstrated that Hsp70 inhibited the aggregation of tau in an isoform-specific fashion, but allowed for robust microtubule assembly. These data, in conjunction with previous studies, indicate that increased Hsp70 levels can inhibit the dysfunction of tau (aggregation) while allowing the normal microtubule assembly and binding function of tau to remain intact, confirming up-regulation of Hsp70 levels/activity as an attractive potential therapeutic for neurodegenerative tauopathies. Additionally, the differences in Hsp70 interactions with tau isoforms, especially 3R vs. 4R, stresses the importance of considering the nature of tau isoforms used in modeling tau neurodegeneration both *in vitro* and *in vivo*.

Supplementary Material

Refer to Web version on PubMed Central for supplementary material.

Acknowledgments

We thank Dr. John Karanicolas and Dr. John Kelly for critically reading this manuscript. We thank James Odum and Akosua Kernizan for their assistance with protein purification.

Abbreviations

AD	Alzheimer's disease
Hsp70	heat shock protein 70
ARA	arachidonic acid
ThS	thioflavin S
LLS	laser light scattering

REFERENCES

1. Himmler A. Structure of the bovine tau gene: alternatively spliced transcripts generate a protein family. Mol Cell Biol. 1989; 9:1389–1396. [PubMed: 2498650]
2. Himmler A, Drechsel D, Kirschner MW, Martin DW Jr. Tau consists of a set of proteins with repeated C-terminal microtubule-binding domains and variable N-terminal domains. Mol Cell Biol. 1989; 9:1381–1388. [PubMed: 2498649]
3. Hernandez F, Avila J. Tauopathies. Cell Mol Life Sci. 2007; 64:2219–2233. [PubMed: 17604998]
4. Lee VM, Goedert M, Trojanowski JQ. Neurodegenerative tauopathies. Annu Rev Neurosci. 2001; 24:1121–1159. [PubMed: 11520930]
5. Boutajangout A, Boom A, Leroy K, Brion JP. Expression of tau mRNA and soluble tau isoforms in affected and non-affected brain areas in Alzheimer's disease. FEBS Lett. 2004; 576:183–189. [PubMed: 15474035]

6. Chambers CB, Lee JM, Troncoso JC, Reich S, Muma NA. Overexpression of four-repeat tau mRNA isoforms in progressive supranuclear palsy but not in Alzheimer's disease. Ann Neurol. 1999; 46:325–332. [PubMed: 10482263]
7. Connell JW, Rodriguez-Martin T, Gibb GM, Kahn NM, Grierson AJ, Hanger DP, Revesz T, Lantos PL, Anderton BH, Gallo JM. Quantitative analysis of tau isoform transcripts in sporadic tauopathies. Brain Res Mol Brain Res. 2005; 137:104–109. [PubMed: 15950767]
8. Goedert M, Spillantini MG, Jakes R, Rutherford D, Crowther RA. Multiple isoforms of human microtubule-associated protein tau: sequences and localization in neurofibrillary tangles of Alzheimer's disease. Neuron. 1989; 3:519–526. [PubMed: 2484340]
9. Goedert M, Spillantini MG, Potier MC, Ulrich J, Crowther RA. Cloning and sequencing of the cDNA encoding an isoform of microtubule-associated protein tau containing four tandem repeats: differential expression of tau protein mRNAs in human brain. Embo J. 1989; 8:393–399. [PubMed: 2498079]
10. Ingelsson M, Ramasamy K, Cantuti-Castelvetri I, Skoglund L, Matsui T, Orne J, Kowa H, Raju S, Vanderburg CR, Augustinack JC, de Silva R, Lees AJ, Lannfelt L, Growdon JH, Frosch MP, Standaert DG, Irizarry MC, Hyman BT. No alteration in tau exon 10 alternative splicing in tangle-bearing neurons of the Alzheimer's disease brain. Acta Neuropathol. 2006; 112:439–449. [PubMed: 16802167]
11. Espinoza M, de Silva R, Dickson DW, Davies P. Differential incorporation of tau isoforms in Alzheimer's disease. J Alzheimers Dis. 2008; 14:1–16. [PubMed: 18525123]
12. Glatz DC, Rujescu D, Tang Y, Berendt FJ, Hartmann AM, Faltraco F, Rosenberg C, Hulette C, Jellinger K, Hampel H, Riederer P, Moller HJ, Andreadis A, Henkel K, Stamm S. The alternative splicing of tau exon 10 and its regulatory proteins CLK2 and TRA2-BETA1 changes in sporadic Alzheimer's disease. J Neurochem. 2006; 96:635–644. [PubMed: 16371011]
13. Lace G, Savva GM, Forster G, de Silva R, Brayne C, Matthews FE, Barclay JJ, Dakin L, Ince PG, Wharton SB. Hippocampal tau pathology is related to neuroanatomical connections: an ageing population-based study. Brain. 2009; 132:1324–1334. [PubMed: 19321462]
14. Shi J, Qian W, Yin X, Iqbal K, Grundke-Iqbal I, Gu X, Ding F, Gong CX, Liu F. Cyclic AMP-dependent protein kinase regulates the alternative splicing of tau exon 10: a mechanism involved in tau pathology of Alzheimer disease. J Biol Chem. 2011; 286:14639–14648. [PubMed: 21367856]
15. Umeda Y, Taniguchi S, Arima K, Piao YS, Takahashi H, Iwatsubo T, Mann D, Hasegawa M. Alterations in human tau transcripts correlate with those of neurofilament in sporadic tauopathies. Neurosci Lett. 2004; 359:151–154. [PubMed: 15050686]
16. Yasojima K, McGeer EG, McGeer PL. Tangled areas of Alzheimer brain have upregulated levels of exon 10 containing tau mRNA. Brain Res. 1999; 831:301–305. [PubMed: 10412011]
17. Voss K, Gamblin TC. GSK-3beta phosphorylation of functionally distinct tau isoforms has differential, but mild effects. Mol Neurodegener. 2009; 4:18. [PubMed: 19409104]
18. Koren J 3rd, Jinwal UK, Lee DC, Jones JR, Shults CL, Johnson AG, Anderson LJ, Dickey CA. Chaperone signalling complexes in Alzheimer's disease. J Cell Mol Med. 2009; 13:619–630. [PubMed: 19449461]
19. Hartl FU, Hayer-Hartl M. Molecular chaperones in the cytosol: from nascent chain to folded protein. Science. 2002; 295:1852–1858. [PubMed: 11884745]
20. Brown IR. Heat shock proteins and protection of the nervous system. Ann. N.Y. Acad. Sci. 2007; 1113:147–158. [PubMed: 17656567]
21. Young JC. Mechanisms of the Hsp70 chaperone system. Biochem Cell Biol. 2010; 88:291–300. [PubMed: 20453930]
22. Chen X, Li Y, Huang J, Cao D, Yang G, Liu W, Lu H, Guo A. Study of tauopathies by comparing Drosophila and human tau in Drosophila. Cell Tissue Res. 2007; 329:169–178. [PubMed: 17406902]
23. Dou F, Netzer WJ, Tanemura K, Li F, Hartl FU, Takashima A, Gouras GK, Greengard P, Xu H. Chaperones Increase Association of Tau Protein with Microtubules. PNAS. 2003; 100:721–726. [PubMed: 12522269]

24. Sahara N, Maeda S, Yoshiike Y, Mizoroki T, Yamashita S, Murayama M, Park J-M, Saito Y, Murayama S, Takashima A. Molecular Chaperone-Mediated Tau Protein Metabolism Counteracts the Formation of Granular Tau Oligomers in Human Brain. Journal of Neuroscience Research. 2007; 85:3098–3108. [PubMed: 17628496]
25. Petrucelli L, Dickson D, Kehoe K, Taylor J, Snyder H, Grover A, De Lucia M, McGowan E, Lewis J, Prihar G, Kim J, Dillmann WH, Browne SE, Hall A, Voellmy R, Tsuboi Y, Dawson TM, Wolozin B, Hardy J, Hutton M. CHIP and Hsp70 Regulate Tau Ubiquitination, degredation, and aggregation. Human Molecular Genetics. 2004; 13:703–714. [PubMed: 14962978]
26. Sarkar M, Kuret J, Lee G. Two Motifs Within the Tau Microtubule-binding Domain Mediate Its Association With the Hsc70 Molecular Chaperone. Journal of Neuroscience Research. 2008; 86:2763–2772. [PubMed: 18500754]
27. Jinwal UK, Miyata Y, Koren J III, Jones JR, Trotter JH, Chang L, O'Leary J, Morgan D, Lee DC, Shults CL, Rousaki A, Weeber EJ, Zuiderweg ERP, Gestwicki JE, Dickey CA. Chemical Manipulation of Hsp70 ATPase Activity Regulates Tau Stability. Journal of Neuroscience. 2009; 29:12079–12088. [PubMed: 19793966]
28. Jinwal UK, O'Leary JC 3rd, Borysov SI, Jones JR, Li Q, Koren J 3rd, Abisambra JF, Vestal GD, Lawson LY, Johnson AG, Blair LJ, Jin Y, Miyata Y, Gestwicki JE, Dickey CA. Hsc70 rapidly engages tau after microtubule destabilization. J Biol Chem. 2010; 285:16798–16805. [PubMed: 20308058]
29. Evans CG, Chang L, Gestwicki JE. Heat shock protein 70 (hsp70) as an emerging drug target. J Med Chem. 2010; 53:4585–4602. [PubMed: 20334364]
30. Patterson KR, Ward SM, Combs B, Voss K, Kanaan NM, Morfini G, Brady ST, Gamblin TC, Binder LI. Heat Shock Protein 70 Prevents both Tau Aggregation and the Inhibitory Effects of Preexisting Tau Aggregates on Fast Axonal Transport. Biochemistry. 2011; 50:10300–10310. [PubMed: 22039833]
31. Andreadis A. Tau splicing and the intricacies of dementia. J Cell Physiol. 2011
32. Brandt R, Hundelt M, Shahani N. Tau alteration and neuronal degeneration in tauopathies: mechanisms and models. Biochim Biophys Acta. 2005; 1739:331–354. [PubMed: 15615650]
33. D'Souza I, Schellenberg GD. Regulation of tau isoform expression and dementia. Biochim Biophys Acta. 2005; 1739:104–115. [PubMed: 15615630]
34. Friedhoff P, von Bergen M, Mandelkow EM, Mandelkow E. Structure of tau protein and assembly into paired helical filaments. Biochim Biophys Acta. 2000; 1502:122–132. [PubMed: 10899437]
35. Liu F, Gong CX. Tau exon 10 alternative splicing and tauopathies. Mol Neurodegener. 2008; 3:8. [PubMed: 18616804]
36. Sergeant N, Delacourte A, Buee L. Tau protein as a differential biomarker of tauopathies. Biochim Biophys Acta. 2005; 1739:179–197. [PubMed: 15615637]
37. von Bergen M, Barghorn S, Biernat J, Mandelkow EM, Mandelkow E. Tau aggregation is driven by a transition from random coil to beta sheet structure. Biochim Biophys Acta. 2005; 1739:158–166. [PubMed: 15615635]
38. Butner KA, Kirschner MW. Tau protein binds to microtubules through a flexible array of distributed weak sites. J Cell Biol. 1991; 115:717–730. [PubMed: 1918161]
39. Goode BL, Chau M, Denis PE, Feinstein SC. Structural and functional differences between 3-repeat and 4-repeat tau isoforms. Implications for normal tau function and the onset of neurodegenerative disease. J Biol Chem. 2000; 275:38182–38189. [PubMed: 10984497]
40. Goode BL, Feinstein SC. Identification of a novel microtubule binding and assembly domain in the developmentally regulated inter-repeat region of tau. J Cell Biol. 1994; 124:769–782. [PubMed: 8120098]
41. von Bergen M, Barghorn S, Li L, Marx A, Biernat J, Mandelkow EM, Mandelkow E. Mutations of tau protein in frontotemporal dementia promote aggregation of paired helical filaments by enhancing local beta-structure. J Biol Chem. 2001; 276:48165–48174. [PubMed: 11606569]
42. von Bergen M, Friedhoff P, Biernat J, Heberle J, Mandelkow E. Assembly of tau protein into Alzheimer paired helical filaments depends on a local sequence motif (306VQIVYK311) forming beta structure. Proc Natl Acad Sci U S A. 2000; 97:5129–5134. [PubMed: 10805776]

43. Carmel G, Mager EM, Binder LI, Kuret J. The structural basis of monoclonal antibody Alz50's selectivity for Alzheimer's disease pathology. J Biol Chem. 1996; 271:32789–32795. [PubMed: 8955115]
44. Carlson SW, Branden M, Voss K, Sun Q, Rankin CA, Gamblin TC. A complex mechanism for inducer mediated tau polymerization. Biochemistry. 2007; 46:8838–8849. [PubMed: 17608454]
45. Chirita CN, Congdon EE, Yin H, Kuret J. Triggers of full-length tau aggregation: a role for partially folded intermediates. Biochemistry. 2005; 44:5862–5872. [PubMed: 15823045]
46. Rankin CA, Sun Q, Gamblin TC. Tau phosphorylation by GSK-3beta promotes tangle-like filament morphology. Mol Neurodegener. 2007; 2:12. [PubMed: 17598919]
47. Rankin CA, Sun Q, Gamblin TC. Pre-assembled tau filaments phosphorylated by GSK-3b form large tangle-like structures. Neurobiol Dis. 2008; 31:368–377. [PubMed: 18588978]
48. Sarthy J, Gamblin TC. A light scattering assay for arachidonic acid-induced tau fibrillization without interfering micellization. Anal Biochem. 2006; 353:150–152. [PubMed: 16620751]
49. Sun Q, Gamblin TC. Pseudohyperphosphorylation causing AD-like changes in tau has significant effects on its polymerization. Biochemistry. 2009; 48:6002–6011. [PubMed: 19459590]
50. Bandyopadhyay B, Li G, Yin H, Kuret J. Tau aggregation and toxicity in a cell culture model of tauopathy. J Biol Chem. 2007; 282:16454–16464. [PubMed: 17428800]
51. DeTure M, Granger B, Grover A, Hutton M, Yen SH. Evidence for independent mechanisms and a multiple-hit model of tau assembly. Biochem Biophys Res Commun. 2006; 339:858–864. [PubMed: 16325769]
52. King ME, Gamblin TC, Kuret J, Binder LI. Differential assembly of human tau isoforms in the presence of arachidonic acid. J Neurochem. 2000; 74:1749–1757. [PubMed: 10737634]
53. Benaroudj N, Triniolles F, Ladjimi MM. Effect of nucleotides, peptides, and unfolded proteins on the self-association of the molecular chaperone HSC70. J Biol Chem. 1996; 271:18471–18476. [PubMed: 8702492]
54. Heuser J, Steer CJ. Trimeric binding of the 70-kD uncoating ATPase to the vertices of clathrin triskelia: a candidate intermediate in the vesicle uncoating reaction. J Cell Biol. 1989; 109:1457–1466. [PubMed: 2571614]
55. Necula M, Kuret J. Electron microscopy as a quantitative method for investigating tau fibrillization. Anal Biochem. 2004; 329:238–246. [PubMed: 15158482]
56. Barron DM, Chatterjee SK, Ravindra R, Roof R, Baloglu E, Kingston DG, Bane S. A fluorescence-based high-throughput assay for antimicrotubule drugs. Anal Biochem. 2003; 315:49–56. [PubMed: 12672411]
57. Bonne D, Heusele C, Simon C, Pantaloni D. 4',6-Diamidino-2-phenylindole, a fluorescent probe for tubulin and microtubules. J Biol Chem. 1985; 260:2819–2825. [PubMed: 3972806]
58. Necula M, Kuret J. A static laser light scattering assay for surfactant-induced tau fibrillization. Anal Biochem. 2004; 333:205–215. [PubMed: 15450794]
59. Winsor C. The Gompertz Curve as a Growth Curve. Proc Natl Acad Sci U S A. 1932; 18:1–8. [PubMed: 16577417]
60. Wilson DM, Binder LI. Free fatty acids stimulate the polymerization of tau and amyloid beta peptides. In vitro evidence for a common effector of pathogenesis in Alzheimer's disease. Am J Pathol. 1997; 150:2181–2195. [PubMed: 9176408]
61. Goedert M, Jakes R, Spillantini MG, Hasegawa M, Smith MJ, Crowther RA. Assembly of microtubule-associated protein tau into Alzheimer-like filaments induced by sulphated glycosaminoglycans. Nature. 1996; 383:550–553. [PubMed: 8849730]
62. Voss K, Gamblin TC. GSK-3β phosphorylation of functionally distinct tau isoforms has differential, but mild effects. Mol Neurodegener. 2009; 4:1–12. [PubMed: 19126211]
63. Akiyama H, Barger S, Barnum S, Bradt B, Bauer J, Cole GM, Cooper NR, Eikelenboom P, Emmerling M, Fiebich BL, Finch CE, Frautschy S, Griffin WS, Hampel H, Hull M, Landreth G, Lue L, Mrak R, Mackenzie IR, McGeer PL, O'Banion MK, Pachter J, Pasinetti G, Plata-Salaman C, Rogers J, Rydel R, Shen Y, Streit W, Strohmeyer R, Tooyoma I, Van Muiswinkel FL, Veerhuis R, Walker D, Webster S, Wegrzyniak B, Wenk G, Wyss-Coray T. Inflammation and Alzheimer's disease. Neurobiol Aging. 2000; 21:383–421. [PubMed: 10858586]

64. Markesbery WR, Carney JM. Oxidative alterations in Alzheimer's disease. Brain Pathol. 1999; 9:133–146. [PubMed: 9989456]

65. McGeer EG, McGeer PL. The importance of inflammatory mechanisms in Alzheimer disease. Exp Gerontol. 1998; 33:371–378. [PubMed: 9762518]

66. Ray WJ, Ashall F, Goate AM. Molecular pathogenesis of sporadic and familial forms of Alzheimer's disease. Mol Med Today. 1998; 4:151–157. [PubMed: 9572056]

67. Aksenov MY, Aksenova MV, Butterfield DA, Geddes JW, Markesbery WR. Protein oxidation in the brain in Alzheimer's disease. Neuroscience. 2001; 103:373–383. [PubMed: 11246152]

68. Patterson KR, Remmers C, Fu Y, Brooker S, Kanaan NM, Vana L, Ward S, Reyes JF, Philibert K, Glucksman MJ, Binder LI. Characterization of prefibrillar Tau oligomers in vitro and in Alzheimer disease. J Biol Chem. 2011; 286:23063–23076. [PubMed: 21550980]

69. Jeganathan S, von Bergen M, Brutlach H, Steinhoff HJ, Mandelkow E. Global hairpin folding of tau in solution. Biochemistry. 2006; 45:2283–2293. [PubMed: 16475817]

70. Santos RX, Correia SC, Wang X, Perry G, Smith MA, Moreira PI, Zhu X. Alzheimer's disease: diverse aspects of mitochondrial malfunctioning. Int J Clin Exp Pathol. 2010; 3:570–581. [PubMed: 20661404]

71. Amniai L, Barbier P, Sillen A, Wieruszeski JM, Peyrot V, Lippens G, Landrieu I. Alzheimer disease specific phosphoepitopes of Tau interfere with assembly of tubulin but not binding to microtubules. Faseb J. 2008

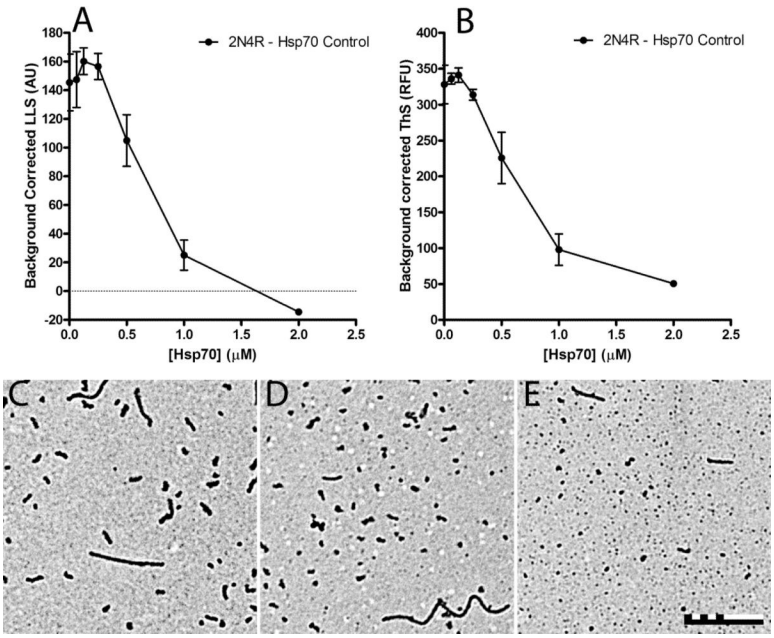

Figure 1. Hsp70 inhibition of arachidonic acid (ARA) induced 2N4R tau aggregation

4 μM 2N4R tau and 150 μM ARA was incubated in the presence of varying amounts of Hsp70 (0-2 μM) for 18 hrs at 37 °C. Aggregation was measured by (A) LLS and (B) ThS fluorescence. Data is in arbitrary units and represents the average equilibrium amounts obtained from 3 trials ± SD with controls for the same reaction without tau subtracted as background for each data point (see Supplemental Figure 1). Representative TEM images are shown for aggregation reactions at (C) 0 μM (no inhibition), (D) 0.5 μM (half maximal inhibition) and (E) 1 μM Hsp70 (maximal inhibition). The scale bar represents 500 nm.

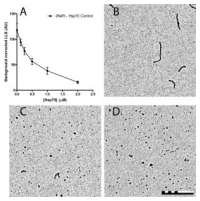

Figure 2. Hsp70 inhibition of Congo red (CR) induced 2N4R tau aggregation

2 μM 2N4R tau and 10 μM CR was incubated in the presence of varying amounts of Hsp70 (0-2 μM) for 18 hrs at 37 °C. Polymerization was measured by (A) LLS. Data is in arbitrary units and represents the average of 3 trials ± SD with controls for the same reaction without tau subtracted as background for each data point (see Supplemental Figure 2). ThS fluorescence could not be used as in Fig. 1 due to CR interference. Representative TEM images are shown for aggregation reactions at (B) 0 μM (no inhibition), (C) 0.5 μM (half maximal inhibition), and (D) 1 μM Hsp70 (maximal inhibition). The scale bar represents 500 nm.

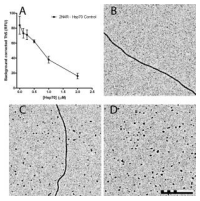

Figure 3. Hsp70 inhibition of heparin induced 2N4R tau aggregation

2 μM 2N4R tau and 6 μg/ml heparin was incubated in the presence of varying amounts of Hsp70 (0-2 μM) for 18 hrs at 37 °C. Aggregation was measured by (A) ThS fluorescence. Data is in arbitrary units and represents the average of 3 trials ± SD with controls for the same reaction without tau subtracted as background for each data point (see Supplemental Figure 3). LLS was not measured as in Figures 1 and 2 due to the very low levels of light scattering that exist with heparin induced aggregation (see Supplemental Figure 3). Representative TEM images are shown for (B) 0 μM (no inhibition), (C) 0.5 μM (half maximal inhibition), and (D) 1 μM Hsp70 (maximal inhibition). The scale bar represents 500 nm.

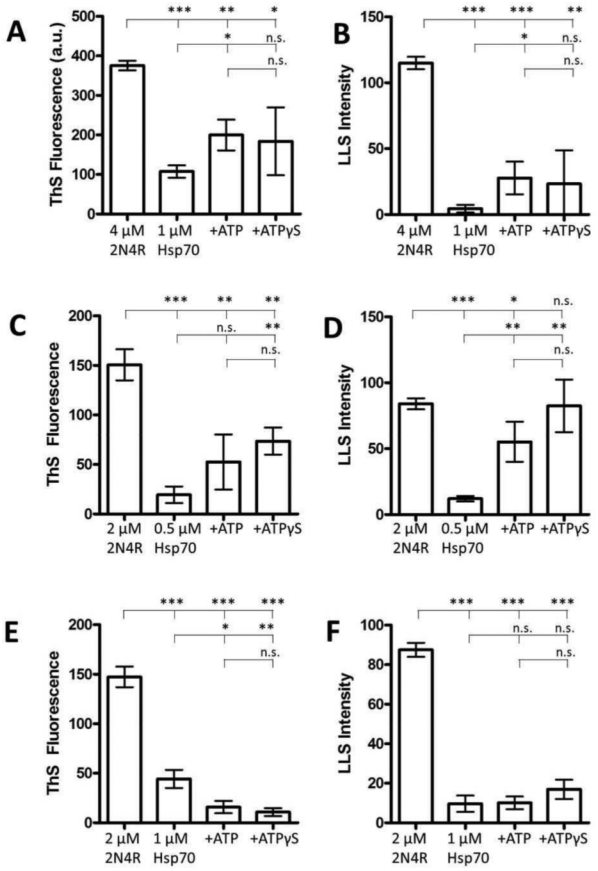

Figure 4. ATP reduces the effect of Hsp70 on tau aggregation

Aggregation of 4 μM 2N4R tau alone, or in the presence of 1 μM Hsp70, 1 μM Hsp70 + 500 μM ATP, or 1 μM Hsp70 + 500 μM ATPγS was measured by ThS fluorescence (A) and LLS (B). Aggregation of 2 μM 2N4R tau alone, or in the presence of 0.5 μM Hsp70, 0.5 μM Hsp70 + 500 μM ATP, or 0.5 μM Hsp70 + 500 μM ATPγS was measured by ThS fluorescence (C) and LLS (D). Aggregation of 2 μM 2N4R tau alone, or in the presence of 1 μM Hsp70, 1 μM Hsp70 + 500 μM ATP, or 1 μM Hsp70 + 500 μM ATPγS was measured by ThS fluorescence (E) and LLS (F). Significant differences (ns = $p > 0.05$, * = $0.01 < p < 0.05$, ** = $0.001 < p < 0.01$, and *** = $p < 0.001$) are denoted with asterisks. Data is in arbitrary units and represent the average of 3 trials ± SD.

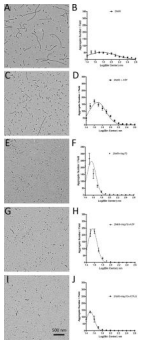

Figure 5. TEM analysis of ATP and Hsp70 effects on tau aggregation

Representative electron micrographs (left) and the transformed aggregate lengths (right) from reactions containing (A, B) 2N4R tau alone, (C, D) 2N4R tau with 500 μM ATP, (E, F) 2N4R tau with 1 μM Hsp70, (G, H) 2N4R tau with 1 μM Hsp70 + 500 μM ATP, and (I, J) 2N4R tau with 1 μM Hsp70 + 500 μM ATPγS. The data is the distribution of five fields per reaction and plotted as the number of aggregates per field versus the log(bin center) and is fit to a Gaussian equation. The scale bar represents 500 nm.

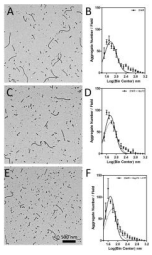

Figure 6. ATP enhances Hsp70 disassembly of pre-formed tau aggregates

4 μM 2N4R tau was induced to aggregate with 150 μM for 6 hrs at 37 °C. Following incubation no additional components (A, B), 1 μM Hsp70 (C, D), or 1 μM Hsp70 with 2 mM ATP (E, F) was added to the reaction for an additional 12 hrs at 37 °C. Reactions were visualized by TEM (A, C, E) and quantitated using Image Pro Plus. The data was transformed to the log scale and the frequency distribution of five fields per reaction was plotted as a function of number of aggregates per field versus the log(bin center) (B, D, F) and fit to a Gaussian equation. The scale bar represents 500 nm. The dashed line in (D) and (F) is the Gaussian fit of 2N4R alone.

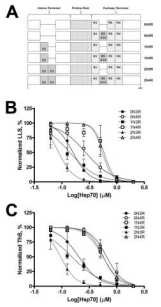

Figure 7. Hsp70 inhibition of ARA induced tau isoform tau aggregation

(A) Schematic of the six tau isoforms used in this study. 4 μM tau isoforms and 150 μM ARA were incubated in the presence of varying amounts of Hsp70 (0-2 μM) for 18 hrs at 37 °C. Aggregation was measured by (A) LLS and (B) ThS fluorescence, with controls for the same reaction without tau subtracted as background for each data point. LLS and ThS values were normalized to the largest observed value as 100% and the lowest observed value as 0% and plotted against the log([Hsp70]). Each data point represents the average of 3 trials ± SD. Isoforms are identified by the symbols as indicated in the key of the graphs.

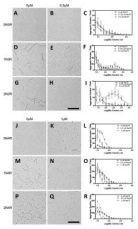

Figure 8. Electron micrographs of Hsp70 inhibited tau isoform aggregation with ARA

Upper panel: representative images are shown for 3R isoforms without Hsp70 (left column, A, D and G), and with Hsp70 at a maximal inhibition concentration (0.5 μM) (right column, B, E and H). Lower panel: representative images are shown for 4R isoforms without Hsp70 (left column, J, M and P), and with Hsp70 at a maximal inhibition concentration (1 μM) (right column, K, N and Q). Scale bars represent 1 μm. Electron micrographs of aggregation reactions performed at three different Hsp70 concentrations corresponding to no inhibition (closed circles), half maximal inhibition (open squares) and maximal inhibition (open circles) were analyzed for aggregate length. Aggregate lengths were transformed to the log scale and binned at an interval of 0.1 nm centers, plotted as the mean of the number of aggregates in a given bin per field ± SD (symbols) of 5 fields and fit to a Gaussian distribution (lines). Graphs for the six isoforms are individually labeled (C – 0N3R; F – 1N3R; I – 2N3R; L – 0N4R; O – 1N4R; and R – 2N4R). The shift in distribution of aggregates towards longer lengths for the 0N4R isoform (L) at the Hsp70 IC_{50} (half maximal inhibition) concentrations was due to aggregate clumping (see Supplemental Figure 5).

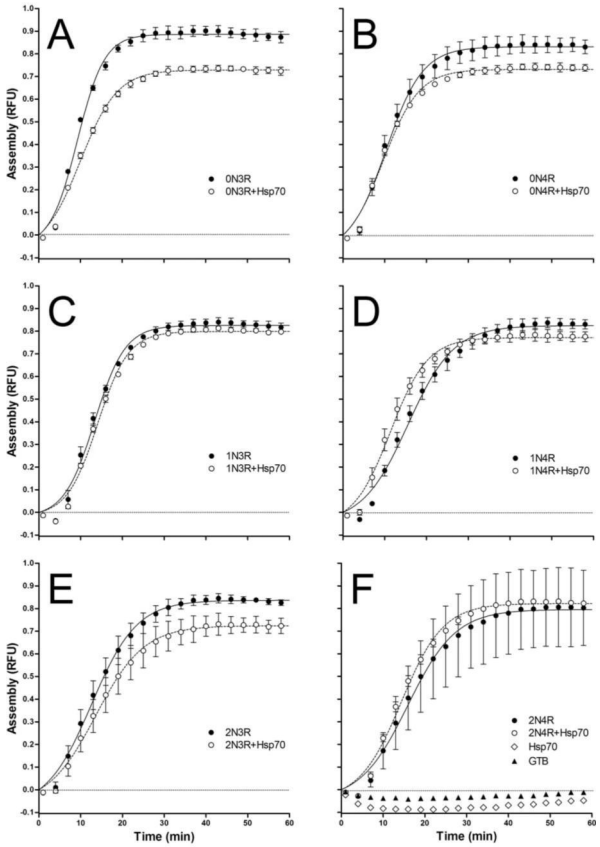

Figure 9. Microtubule assembly with tau isoforms and Hsp70

1 μM tau isoforms were incubated with 1 μM tubulin in the presence (○) or absence (●) of 1 μM Hsp70 at 37 °C. Fluorescent readings at 355 nm excitation and 460 nm emission were taken every minute for 1 hr. Graphs for the six isoforms are individually labeled. Data shown is every other minute for ease of viewing and is plotted as the mean ± SD of 3 trials. Control reactions for tubulin with 1 μM Hsp70 (◇) or tubulin with buffer alone (▲) are shown in (F). The straight dashed line in each graph indicates 0 RFU.

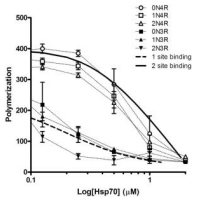

Figure 10. Hsp70 binding models

Hsp70 inhibition of 3R and 4R isoforms are redrawn from Figure 7B and overlaid with simulated data using a 1 site binding equation (dashed black line) and a 2 site binding equation (solid black line). Details for obtaining the fits to the data are provided in Materials and Methods.

Table 1

IC_{50} values for Hsp70 inhibition of tau isoforms ARA induction of polymerization

	IC_{50} Hsp70, μM	
	ThS	**LLS**
0N3R	0.20 ± 0.03	0.16 ± 0.02
1N3R	0.15 ± 0.01	0.14 ± 0.01
2N3R	0.09 ± 0.01	0.09 ± 0.01
0N4R	0.67 ± 0.07	0.26 ± 0.04
1N4R	0.57 ± 0.04	0.64 ± 0.16
2N4R	0.56 ± 0.05	0.55 ± 0.04

Concentration of Hsp70 (in μM) required to inhibit the maximum ARA-induced tau isoform polymerization by 50% (IC_{50}) was determined by fitting ThS and LLS data to a normalized inhibitory dose-response variable slope curve. Data given is the mean ± SD of 3 trials.

Table 2

Statistics of microtubule assembly with tau isoforms and Hsp70.

	Hsp70	Y_{max} (RFU)	K_{app} (min^{-1})	Lag (min)
0N3R	-	0.88 ± 0.01	0.24 ± 0.01	3.72 ± 0.03
	+	0.72 ± 0.01*	0.19 ± 0.00*	3.27 ± 0.05*
1N3R	-	0.82 ± 0.01	0.20 ± 0.00	6.18 ± 0.42
	+	0.79 ± 0.00	0.19 ± 0.00	6.76 ± 0.06
2N3R	-	0.83 ± 0.01	0.15 ± 0.01	4.25 ± 0.41
	+	0.72 ± 0.02*	0.14 ± 0.01	4.66 ± 0.37
0N4R	-	0.82 ± 0.02	0.19 ± 0.01	3.58 ± 0.22
	+	0.72 ± 0.01*	0.19 ± 0.01	3.19 ± 0.13
1N4R	-	0.82 ± 0.01	0.14 ± 0.00	6.05 ± 0.13
	+	0.77 ± 0.01*	0.18 ± 0.01*	4.21 ± 0.30*
2N4R	-	0.79 ± 0.10	0.13 ± 0.01	6.19 ± 0.34
	+	0.82 ± 0.00	0.15 ± 0.00	5.59 ± 0.14

Microtubule polymerization data were fit to the Gompertz growth curve to analyze the lag time, k_{app} (proportional to rate), and maximum polymerization. Data are the average of 3 independent trials ± SD. The asterisk denotes statistical significance at $p<0.05$.